

1

Neuronal Model of Decision Making

Benoit Gaillard, Jianfeng Feng and Hilary Buxton

No Institute Given

Summary. We have built a neuronal model of decision making. Our model performs a decision based on an imperfect discrimination between highly mixed stimuli, and expresses it with a saccadic eye movement, like real living beings. We use populations of integrate-and-fire neurons.

To take a decision that depends on imperfectly separated stimuli, we use a model inspired by the principle of accumulation of evidence. More precisely, this accumulation of evidence is performed by a competition between groups of neurons that model a visual column in the lateral intra-parietal area (area LIP) of the brain. In this column, we have groups of neurons that are sensitive to specific stimuli on which the decision is based. They inhibit each other through groups of inhibitory neurons. Simultaneously, they recursively excite themselves through recurrent synaptic excitation, and all the neurons receive a steady low-level excitation from the rest of the brain. The competition is generated by these recurrent inhibitory and excitatory loops. We study this structure within the framework of dynamical systems. The variables we use are the activities of each group of neurons. This dynamical system has several stable states: one of them occurs when all activities are weak, and other ones when one local group of neurons has a higher activity and dominates the others through lateral inhibition. The convergence to one of these stable states models decision making, guided by sensory evidence. The group of neurons sensitive to the specific stimulus has a comparative advantage on the others during the competition. This structure is not a new idea, but we use it to test our hypothesis on the way the brain controls the dynamics of decision making. Our hypothesis is that the statistical signature of the low-level activity of the brain modifies the stability of the attractors of our model, and thus changes the dynamics of the competition that models decision making.

The criterion by which we judge that a decision is taken is more realistic than just looking at the decisive neurons' activities. We model a saccadic eye movement directed by the activities of our LIP neurons, and we read the decision from the position of the eye. This experimental setup is comparable to biophysical experiments in which living beings express their decisions by saccadic eye movements.

The neurons of the LIP column in which the decisions take place are modeled as neurons in a real brain: besides the stimuli and the recurrent interactions, they receive significant inputs from the rest of the brain. It is well known that neurons in the brain are highly influenced by this activity, called low-level background activity.

We study how the dynamics of the decision making change as a function of the first-order statistics (mean) and second-order statistics (variance) of this global low-level background activity or noise. By studying its influence on the reaction time and error rate, we show that this background activity may be used to control the dynamics of decision making. We compare the performance of such a model (error rate as a function of reaction time) to the performance of living beings during psychophysical experiments. By doing so, we assess the plausibility of the hypothesis that decisions be controlled by the statistical signature of the low-level background activity of the brain.

1.1 Introduction

The study of the reaction time (RT) and error rate (ER) of animals and humans performing a simple two-choice perceptual discrimination task has a long history. One of the first approaches to model such decision processes was developed by psychologists and is known as the accumulation of evidence models. Typically, these models consider two variables that measure the quantity of evidence for each of the two decisions, and the first variable that reaches a decision boundary determines the decision. Those models were introduced by, for example Townsend and Ashby [17]. The diffusion model is often used to explain relations among RT, accuracy, error trials, and clarity of the input. Thanks to successful neural recording during decision making (for example, Shadlen and Gold [14], Platt and Glimcher [12]), experimental evidence confirmed that the diffusion model can account for the accumulation of evidence, but also inspired more precise models of the neural dynamics involved. In particular, accumulation of evidence through neural competition has been modeled by Wang [20] and by Brunel (Amit and Brunel [1]). Glimcher [9] reviews stochastic decision making. According to Glimcher, who tested this claim by experimenting on monkeys, the tendency to make a choice is implemented in the firing rate (FR) of area LIP and the uncertainty about this decision could be implemented by what we call input noise in area LIP. However, decision making is also controlled by our context, our motivations, and our history. This idea has been addressed by Salinas [13]. He uses, as well, background synaptic activity as a switch between dynamical states in a network. We propose a model in which sensory inputs do not automatically trigger a decision. The decision making is dependent on the characteristics of the low-level background neuronal activity of the brain. This background activity does not only control if a decision is taken, but controls the trade-off between speed and accuracy as well: in urgent situations, we tend to take less accurate decisions.

We restrict ourselves to a very simple decision in the case of very simple and well-studied sensory evidence setup. We use moving-dot kinematograms as stimuli, and the model has to decide in which direction to move its eye, signifying if it thinks that the dots generally move downwards or upwards. This experimental setup has been extensively studied on alive monkeys and on humans by Newsome and colleagues ([2, 15, 16, 21]. Our moving-dot kinematograms are composed of a hundred dots. A percentage of them move coherently in one direction. This percentage is called coherence in this chapter. The rest of them move randomly in any direction. In our experimental setups, they don't even have consistent directions. This setup is the same as in previous studies [3, 5, 6], and as in many of Newsome's experimental setups.

We currently treat these stimuli in a very crude way. We suppose that the retina and the early parts of the visual system evaluate the direction of each dot during successive short time steps. Authors have argued for such a discretization of time in the visual system (VanRullen and Koch [19]). We suppose that each dot moving in a given direction triggers the activity of specific motion detectors. There are more detailed models that support this idea: It has been proved that in the visual system, we find columns of neurons that detects specific directions of movement (Mountcastle [11] Hubel and Wiesel [10]). So we suppose that the first detailed neurons of our model receive a hundred different synaptic inputs, each of these inputs corresponding to the direction of one dot. These neurons are detectors of the global direction of the dots in the kinematogram: they react strongly to a given general direction and weakly to its opposite direction. To implement this neural behaviour, we set their synaptic input to be inversely proportional to the difference between their preferred direction and the direction of the corresponding dot.

These global direction detectors and the rest of the model is described more precisely in this chapter.

1.2 Model

1.2.1 Overview

Our model can be divided into three parts, illustrated in Figure 1.1. First we have the global direction detectors. They are made of populations of integrate-and-fire (IF) neurons whose firing rates (FRs) depend on the global direction of the dots in the stimulus. They are a very simple generalisation of the model we studied in earlier publications [6, 7]. Using the output of the direction detectors, we have our LIP decisive column. Internal recursive loops and global inputs from the brain determine the activities of the neurons in the column. Specific patterns of activity of this column can generate an eye movement.

The generation of this eye movement is the third part of the model.

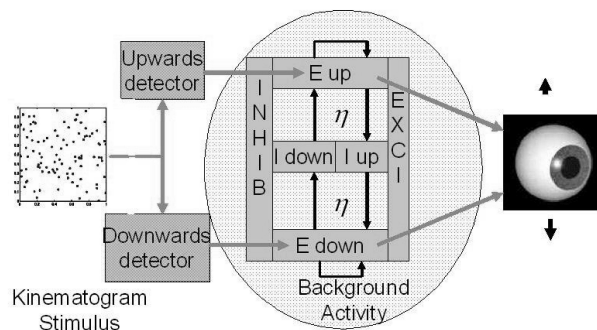


Fig. 1.1. The left panel represents the stimulus: Normally all those dots are moving, most of them randomly. The middle panel is an illustration of the neuronal activities in the decision column of area LIP. In the middle panel, we see the low-level background activity of the brain (represented by the green colour) that surrounds the column. All the represented subpopulations of neurons are connected to themselves and to each other, but the arrows represent Hebbian learning-potentiated connections. When the eye on the right has turned to one side, a decision has been taken.

The neuron model used here is the classic leaky integrate-and-fire (IF) model [4, 8, 18]. The dynamics of the membrane potential below threshold are defined as follows:

$$dV = -\frac{1}{\tau}(V - V_{rest})dt + dI_{syn}(t) \quad (1.1)$$

where τ is the time constant of the neuron and the synaptic input is

$$I_{syn}(t) = \sum_{i=1}^{N_s} a_i E_i(t) \quad (1.2)$$

where $E_i(t)$ is the instantaneous frequency of incoming spikes to the i^{th} synapse, a_i is the positive or negative magnitudes of the excitatory postsynaptic potential (EPSP) and the inhibitory postsynaptic potential (IPSP) respectively, and N_s is the number of synapses. When the membrane potential reaches V_θ , the threshold potential, the neuron emits a spike and the potential is reset to V_{rest} . Then, the neuron goes through a refractory period τ_{ref} during which its membrane potential remains close to V_{rest} . We assume that large groups of incoming synapses receive the activity of large populations of neurons that have a similar activity, and that this activity is small. In that case, as shown by Tuckwell [18], we can use the diffusion approximation. So we can rewrite Eq. (1.2) as

$$I_{syn}(t) = J \sum_{i=1, w_i > 0}^{N_g} w_i \nu_i(t) - J_{inh} \sum_{i=1, w_i < 0}^{N_g} w_i \nu_i(t)$$

- N_g is the number of groups of similar incoming synapses to the neuron.
- w_i is the normalized synaptic weight. It is negative for inhibitory synapses.
- ν_i is the rate of the Poisson process coming to the synapses of the group i .
- J is the global excitatory synaptic strength.
- J_{inh} is the global inhibitory synaptic strength.

Then we reach the following expression for the output FR:

$$\nu_{out} = \left[\tau_{ref} + \tau \int_{\frac{V_{rest}-\mu}{\sigma}}^{\frac{V_\theta-\mu}{\sigma}} \phi(u) du \right]^{-1} \quad (1.3)$$

where

$$\phi(u) = \sqrt{\pi} e^{u^2} (1 + erf(u))$$

$$\mu = J \sum_{i=1}^{N_g} w_i \nu_i$$

$$\sigma^2 = J^2 \sum_{i=1}^{N_g} w_i^2 \nu_i + J^2 \sum_{i,j=1, i \neq j}^{N_g} c_{i,j} w_i w_j \sqrt{\nu_i \nu_j}$$

- $c_{i,j}$ is the correlation coefficient between synapse group i and synapse group j . We assume that the correlation coefficient between the inhibitory and excitatory synapse is zero.
- The resting membrane potential: $V_{rest} = 0$ mV.
- The threshold membrane potential: $V_\theta = 20$ mV.
- τ_{ref} is the refractory period of the leaky integrate-and-fire neuron.
- τ is the time constant of the leaky integrate-and-fire neuron.

1.2.2 Global Direction Detectors

The global direction detectors are constituted of populations of leaky integrate-and-fire neurons described in the previous section. Each detector is made of 100 such neurons that are not laterally connected and that receive the same input. The discrimination of such a population is quicker and more accurate, as shown in previous publications (Gaillard et al. [6, 7]). We do not evaluate statistically the output FR of the neuron, as in Eq. (1.3), but we simulate the production of spikes. For one time window t , the population produces N spikes, and the firing rate is $\frac{N}{100t}$.

The synaptic excitation is basically inversely proportional to the distance between the preferred angle of the group and the stimulus angle. Keeping the paradigm of one group of synapses for one dot, synaptic excitation for the upward detector will be π for a dot moving upward, 0 for a dot moving downward, and $\frac{\pi}{2}$ for a dot moving horizontally.

$$\nu_i = k \|(\|Angle - Direction_i\| + \pi)[2\pi] - pi\|$$

where ν_i is the incoming rate corresponding to i^{th} dot number, $Angle$ is the preferred direction of the detector, $Direction_i$ is the moving dot's direction, and k is a normalizing parameter, so that the excitation stays in the range of rates used in our experimental models. This equation is justified by the idea that the direction detector has more synaptic connections to the motion detector of its preferred direction. We assume as well that the incoming activity corresponding to dots having a coherent direction is correlated. n_c is the number of dots moving coherently, and c is the correlation coefficient. For simplicity, we assume that the detector's synaptic characteristics are as follows: the magnitude (a_i) of an EPSP is the exact opposite of the magnitude of an IPSP, and has the same absolute value for all synapses: a . r is the ratio between the number of excitatory and inhibitory synapses of the Direction Detector. Thus, as shown by Tuckwell [18], we can simplify Eq. (1.1) into:

$$dV = -\frac{1}{\tau}(V - V_{rest})dt + \mu dt + \mathcal{N}\sigma\sqrt{dt}$$

where

$$\begin{aligned}\mu &= a \sum_{j=1}^p (1-r)\nu_j; \\ \sigma^2 &= a^2 \left[\sum_{j=1}^p (1+r)\nu_j + \sum_{i,j=1, i \neq j}^{n_c} c(1+r)\sqrt{\nu_i\nu_j} \right]\end{aligned}\quad (1.4)$$

- r is the ratio between inhibitory synapses and excitatory synapses.
- $p = 100$ is the number of groups of synapses that receive inputs corresponding to the direction of one dot.
- $\nu(j)$ is the incoming rate corresponding to the direction of the j^{th} dot.
- The time constant of the neuron: $\tau = 20$ ms.
- The time step for the integration: $dt = 0.01$ ms.
- The correlation coefficient between inputs from dots that have a coherent motion: $c = 0.1$.
- The number of coherent inputs: $n_c \leq p$. Coherent inputs are dots that move consistently in one direction.
- The resting membrane potential: $V_{rest} = 0$ mV.
- The threshold membrane potential: $V_{threshold} = 20$ mV.
- \mathcal{N} is a normally distributed random variable (mean 0, variance 1); in the formal IF model, $\mathcal{N}\sqrt{dt}$ is the standard Brownian motion.

Characteristics of This Model

We previously studied this model (Gaillard et al. [6, 7]). We showed that the discrimination accuracy is better when the ratio r between excitatory and inhibitory inputs is closer to $r = 1$. We showed that the population coding reduces considerably the time needed to evaluate the firing rate, and increases the discrimination accuracy. The FR decreases with r . However, to obtain a reliable measure of the FR, we need to produce at least 100 spikes. Thus, in our model, in order to take decisions faster, we use $r = 0$.

The output FR of the direction detector is used as the specific inputs of the competing groups of neurons in area LIP. These competing groups of neurons form the column that is described in the next subsection.

Figure 1.2 shows that the mean FR increases linearly with the coherence, as assumed in Wang [20]. The output of our detectors actually fits his assumption of a Gaussian distribution of rates very well. We used this approximation to measure the TPM in our paper [7].

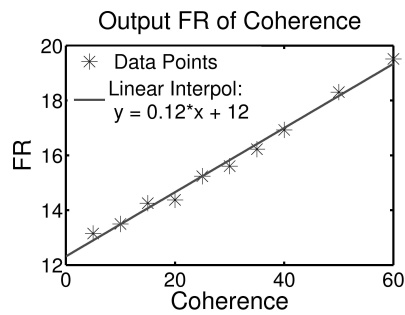


Fig. 1.2. The firing rate of a motion detector as a function of the coherence of the stimulus. The global direction of the stimulus is the preferred one of the detector. It is a linear relationship.

1.2.3 LIP Column: Where The Decision Is Made

Column Organisation

If we have p specific stimuli, then our column is described by $2p + 2$ subpopulations of neurons:

- p subpopulations of excitatory neurons specifically sensitive to the specific stimuli
- one subpopulation of nonspecific excitatory neurons
- one subpopulation of nonspecific inhibitory neurons

- p subpopulations of specific inhibitory neurons. They are specifically connected to the specific excitatory neurons, and specifically inhibit populations of neurons.

The specific connections between neurons are modeled to have arisen through Hebbian learning, η being the learning coefficient, or long-term potentiation coefficient. The rest of the synapses are depressed, to keep a normalized synaptic strength.

This leads us to the following parameters:

- $x (= 0.8)$: the fraction of local module synapses relatively to external input.
- $J (= 11)$: synaptic excitatory unstructured strength to one neuron.
- $C (= 1.01)$: inhibitory synaptic strength is slightly stronger than excitatory; this is a stability condition. (I have the formal proof of it in one dimension, Amit and Brunel [1] showed it as well).
- $\eta (= 9)$: learning coefficient.
- $f (= 0.01)$: proportion of neurons specifically sensitive to a specific stimulus.
- $p (= 2)$: number of specific stimuli.
- $f_i (= 0.1/p)$: proportion of inhibitory neurons specifically sensitive to a subpopulation of excitatory neurons.
- $\eta^- = \max(0, \frac{1-\eta \times f}{1-f})$: synaptic depression.
- $C^- = \max(0, \frac{C*(1-\eta \times f_i)}{1-f_i})$: synaptic depression of inhibitory synapses to an excitatory neuron.
- ξ : standard deviation of the external background activity. This standard deviation varies spatially and temporally.
- $f_b (= 2/3)$: relative strength of the background activity in comparison to the whole external input.
- $f_1 = f_2 = \dots f_p = \frac{1-f_b}{p}$: relative strength of each specific input in comparison to the whole external input.

The learning rule is expressed as follows: Since neurons that are more sensitive to a specific stimulus will more often fire together, their connection will be strengthened. We express it: $J^+ = \eta \times J$, where J is the average unstructured synaptic strength. The rest of the synapses will be depressed, so that the mean synaptic strength remains J . Thus, in our case, we have: $\eta^- = \max(0, \frac{1-\eta \times f}{1-f})$. We truncated the synaptic strength so that it cannot be a negative strength, as seen in biology. We also suppose learning between inhibitory neurons. Our assumption is that some inhibitory neurons will show self-organisation properties, strengthen their incoming synapses from subpopulations of excitatory neurons, and fire correlatively. This learning parameter will be the same, η , and the synaptic depression will be similar.

We can concisely represent the structure of the column with the following matrix A . Each element $A_{i,j}$ of the matrix represents the strength of the

influence of the neurons of group j on the neurons of group i . This is the synaptic strength of each synapse, multiplied by the number of synapses.

$$A = (M, N)$$

Where

$$M =$$

$$M = \begin{pmatrix} xf\eta & xf\eta^- & -xf_iC^- & -xf_i\eta C & -x(1-pf_i)C & x(1-pf)\eta^- \\ xf\eta^- & xf\eta & -xf_i\eta C & -xf_iC^- & -x(1-pf_i)C & x(1-pf)\eta^- \\ xf\eta & xf\eta^- & -xf_iC & -xf_iC & -x(1-pf_i)C & x(1-pf)\eta^- \\ xf\eta^- & xf\eta & -xf_iC & -xf_iC & -x(1-pf_i)C & x(1-pf)\eta^- \\ xf & xf & -xf_iC & -xf_iC & -x(1-pf_i)C & x(1-pf) \\ xf & xf & -xf_iC & -xf_iC & -x(1-pf_i)C & x(1-pf) \end{pmatrix}$$

$$N = \begin{pmatrix} (1-x)f_b(1+\xi\mathcal{N}) & (1-x)f_1 & 0 \\ (1-x)f_b(1+\xi\mathcal{N}) & 0 & (1-x)f_2 \\ (1-x)f_b(1+\xi\mathcal{N}) & 0 & 0 \end{pmatrix}$$

System Equations

We use a discrete formalism. At each time step, we reevaluate the variables of the system (rates of the output Poisson processes), as a function of their value at the previous time step, and of the value of the contextual variables. The contextual variables are the external inputs: global activity of the brain, and direction detector activity.

$$\nu_{n+1}^{int} = F(\nu_n^{int}, \nu_n^{ext}) \quad (1.5)$$

where

$$F(\nu_n^{int}, \nu_n^{ext}) = \left[\tau_{ref} + \tau \int_{\frac{\nu_{rest}-\mu}{\sigma}}^{\frac{\nu_\theta-\mu}{\sigma}} \phi(u) du \right]^{-1}$$

where

- $\phi(u) = \sqrt{\pi}e^{u^2}(1 + erf(u))$.
- $\mu = \mu(\nu_n^{int}, \nu_n^{ext})$ is described in the next subsections.
- $\sigma = \sigma(\nu_n^{int}, \nu_n^{ext})$ is described in the next subsections.
- ν^{int} is the vector representing the output rates of the neurons in the column.

$$\nu^{int} = \begin{pmatrix} \nu_{up} \\ \nu_{down} \\ \nu_{i,up} \\ \nu_{i,down} \\ \nu_i \\ \nu_0 \end{pmatrix}$$

- ν^{ext} is the vector representing the output rates of the neurons in the brain and the direction detectors.

$$\nu^{ext} = \begin{pmatrix} \nu_{global} \\ \nu_{ext,up} \\ \nu_{ext,down} \end{pmatrix}$$

- $\tau_{ref} = 0.0005$ refractory period in seconds.
- $\tau = 0.05$ neuronal time constant in seconds.

The Variable μ

In equation Eq. (1.2), the relation between μ and the incoming Poisson rate is linear. So we can write this $(2p+5)$ linear equation:

$$\mu = J \times A \times \nu \quad (1.6)$$

where μ is a vector of size $(2p+2)$, representing the various subpopulations of neurons in the LIP column. ν_n is a vector of size $(2p+5)$, representing the rate of the Poisson processes received from the various subpopulations of neurons. ν is the combination of ν^{ext} and ν^{int} . A is a matrix of size $(2p+2) \times (2p+5)$. If we take the example of $p = 2$, for the two choices of the dot direction decision

task (upward or downward), we have: $\mu = \begin{pmatrix} \mu_{up} \\ \mu_{down} \\ \mu_{i,up} \\ \mu_{i,down} \\ \mu_i \\ \mu_0 \end{pmatrix}, \nu = \begin{pmatrix} \nu_{up} \\ \nu_{down} \\ \nu_{i,up} \\ \nu_{i,down} \\ \nu_i \\ \nu_0 \\ \nu_{global} \\ \nu_{ext,up} \\ \nu_{ext,down} \end{pmatrix}$

The Variable σ

Currently, we suppose that the correlation between neurons that belong to the same group (for example, the group of excitatory neurons that is especially

sensitive to the upward direction detector) is $c = 0.1$. The correlation between neurons of two different groups is $c = 0.01$. The correlation between inhibitory and excitatory neurons is $c = 0$. So, in the particular case that we study here ($p = 2$), we obtain the following correlation matrix:

$$c = \begin{pmatrix} 0.1 & 0.01 & 0 & 0 & 0 & 0.01 & 0.01 & 0.01 & 0.01 \\ 0.01 & 0.1 & 0 & 0 & 0 & 0.01 & 0.01 & 0.01 & 0.01 \\ 0 & 0 & 0.1 & 0.01 & 0.01 & 0 & 0 & 0 & 0 \\ 0 & 0 & 0.01 & 0.1 & 0.01 & 0 & 0 & 0 & 0 \\ 0 & 0 & 0.01 & 0.01 & 0.1 & 0 & 0 & 0 & 0 \\ 0.01 & 0.01 & 0 & 0 & 0 & 0.1 & 0.01 & 0.01 & 0.01 \\ 0.01 & 0.01 & 0 & 0 & 0 & 0.01 & 0.1 & 0.01 & 0.01 \\ 0.01 & 0.01 & 0 & 0 & 0 & 0.01 & 0.01 & 0.1 & 0.01 \\ 0.01 & 0.01 & 0 & 0 & 0 & 0.01 & 0.01 & 0.01 & 0.1 \end{pmatrix}$$

Consequently, for a neuron belonging to group n , we have

$$\sigma_n^2 = \frac{1}{2} J^2 \left(\sum_{i=1}^{N_g} A_{n,i}^2 \nu_i + \sum_{i,j=1, i \neq j}^{N_g} c_{i,j} A_{n,i} A_{n,j} \sqrt{\nu_i \nu_j} \right) \quad (1.7)$$

Where

- N_g is the number of group of neurons.
- A is the matrix seen before.
- $c_{i,j}$ is the correlation coefficient between the i^{th} and the j^{th} synapses.

1.2.4 Saccadic Eye Movement

To express the decision, we model a saccadic eye movement (SEM). This is the paradigm that is used in Newsome's lab to evaluate the decisions of monkeys during the same task. In our model, the eye position is governed by the following equation:

$$\frac{\partial x}{\partial t} = k \times R - l \times \tan(x)$$

- x represents the angular position of the eye.
- k and l are parameters. In our recent experiments: $k = l = 3$.
- R is the input that comes from the LIP column. In the two-dimensional case ($p = 2$), $R = \nu_{up} - \nu_{down}$.

The term $\tan(x)$ models an elastic force that tends to bring the eye in its central position if no specific command is sent, and that also prevents the eye's angular position from diverging. In fact, when x tends to $\frac{\pi}{2}$, the force modeled by $\tan(x)$ tends to ∞ , thus the moving span of the eye is limited. The position of the eye gives us a natural criterion to measure ER and RT. At the moment, we consider that a decision is made when $x = 0.95\frac{\pi}{2}$.

1.3 Results/Predictions

1.3.1 Methods

We ran a set of experiments, covering the parameter space that follows: The mean of the global background activity varied from 3 to 10 Hz, and the standard deviation varied from 0 to 5 Hz. We measured the reaction time and error rate of the model. For each parameters combination, we averaged the results over 10 repetitions. All simulations were conducted with stimuli that had 5% coherence.

1.3.2 Time Course of Decision: Convergence to a Local Attractor

Figure 1.3 illustrates the time course of decision making. We can see the competition that leads to the convergence to a local attractor, along with the eye position over time. We see as well that the recurrent loops enable the model to keep in mind the decision even when the stimulus disappears. We can argue that we are implementing here a kind of working memory. In fact this decision is not expressed by the model until the difference of activity between the two populations has been consistent enough for the eye to have accomplished its saccadic movement. We see in Figure 1.3 that the decision is kept in memory, because we have artificially reset the eye in the middle position when the stimulus stopped. However, the system stays in the attractor, and when the eye is released it expresses the delayed decision.

1.3.3 Background Activity Controls Decision Making

Mean Intensity of the Background Activity

Reaction Time

We clearly see in Figure 1.4 that increasing the intensity of the background activity reduces the reaction time. We can still see the ‘switch’ effect described by Salinas [13]: If the background activity tends to zero, then the reaction time tends to infinity. This switch effect is part of a more global control exerted by the external activity on the decision process.

Error Rate

The error rate increases with the intensity of the background activity following a sigmoid function. In Figure 1.5, we can see a four parameter exponential approximation of this increase.

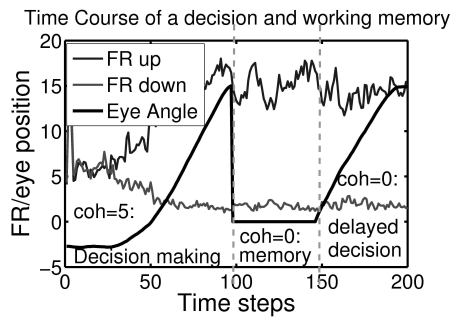


Fig. 1.3. Illustration of decision making and working memory. The stimulus is presented during the first 100 time steps. Then, the eye is reset to the middle position and the stimulus disappears (100 to 150). However, we see that the decision is maintained when we free the eye and the system expresses a delayed decision.

$$\text{Error Rate} = F(\text{Reaction Time})$$

Figure 1.6 shows the characteristic of ER as a function of RT, deducted from the previous results. This was possible because RT is a monotonically increasing function of background intensity. This result is important because it is prediction of the model and gives us a tool to evaluate our hypothesis that background activity controls the speed/accuracy trade-off in decision making: If, during psychological experiments, humans show a similar dependency between ER and RT, then our model for the underlying process is likely to be plausible.

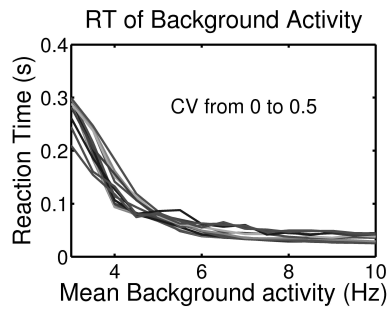


Fig. 1.4. Reaction time as a function of the mean intensity of the background activity of the brain. The decision processes were stopped after 0.3 seconds, to reduce computational time. In fact, if no decision is made, when the background activity is too weak, RT tends to infinity.

Standard Deviation of the Background Activity

Reaction Time

Figure 1.7 shows that the real noise also speeds up decision making. In this simulation, the mean of the low-level background activity is constant. Its standard deviation is the only parameter that varies. This is a new result, purely based on the second-order moment of the brain's stochastic neural activity.

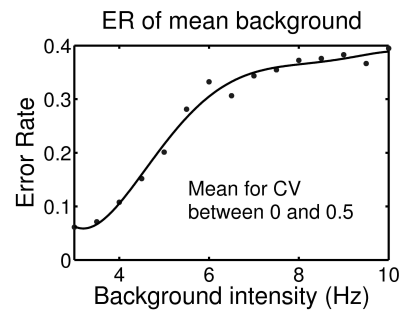


Fig. 1.5. Error rate as a function of the mean intensity of the background activity of the brain. This is an average over all the values of the standard deviation, between 0 and 5.

Error Rate

Figure 1.8 shows a significant influence of noise on the error rate. For each value of the standard deviation, we have measured the ER for the range of mean background intensities, and then taken the mean over all these simulations.

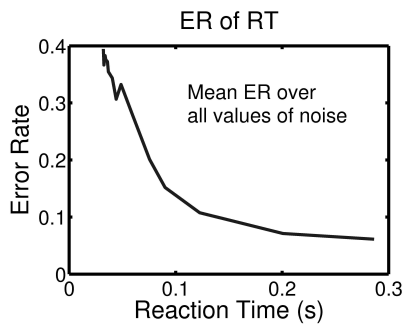


Fig. 1.6. ER as a function of the RT. Our method is basically a change of variables from the mean background activity to the RT. This works because we have seen previously that the RT is a monotonic function of the background intensity. Here, we have taken the mean over all the values of the standard deviation of the background activity.

1.4 Discussion

1.4.1 Summary of the Results

We have implemented a model that performs decision making and expresses it through a saccadic eye movement. This is a step forward from the models in which the external observer has to watch a neural variable, because we can use measures such as the reaction time and error rate of our model in order to compare it to living being's performance. We have shown that the

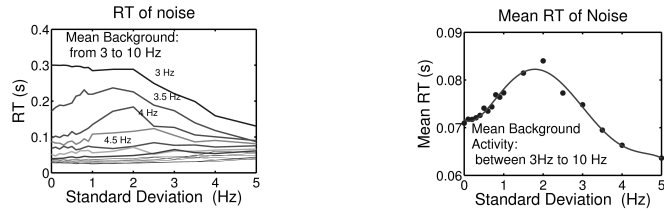


Fig. 1.7. Reaction time as a function of the standard deviation of the background activity. In the first panel, the mean activity varies between 3 Hz and 10 Hz. The second panel is the mean function, averaged over the whole range of background mean intensities (it is the average of the curves presented in the first panel).

low-level noisy background activity of the brain can be beneficial to decision making, in the case of very ambiguous sensory evidence. We have reproduced the results of Salinas that an increase in the mean of the low-level background activity can trigger decision making. We went much further than this intuitive result (if you add more energy in a competitive system, the convergence to the outcome will be quicker). We explored quantitatively the influence of the background intensity on the reaction time and on the error rate, and deduced a relation between error rate and reaction time. Furthermore we showed that an increase in the actual noisy property of the background activity, without an increase of its mean, also speeds up decision making at the cost of accuracy. This is a new result.

1.4.2 Limitations

The parameter space is huge. We only explored a small region. The results are dependent on the SEM model, which is currently over simplistic and has not been compared to biological evidence. We only have simulations.

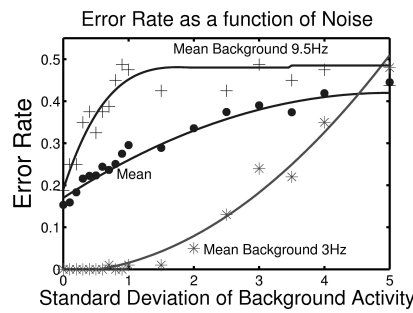


Fig. 1.8. Error rate as a function of the standard deviation of the background activity of the brain. There are three different behaviours for three different mean intensities of the background activity.

1.4.3 Developments

Moment Mapping

The second-order statistics are fundamental to the results we presented here. However, we have assumed that the spikes are emitted according to Poisson processes. That means that the presynaptic noise is proportional to its mean, and enables us to write Eq. (1.4), and gives us Eq. (1.5) as an equation for the propagation of the first moment of the interspike interval (ISI) distribution. However, this assumption does not hold in the general case, and furthermore

there is little biological evidence for LIP neuronal activity to be Poissonian. So, we have a more general expression than Eq. (1.5). In the general case:

$$(\nu_{n+1}^1, \nu_{n+1}^2) = G(\nu_n^1, \nu_n^2) \quad (1.8)$$

where ν_{n+1}^1 and ν_{n+1}^2 are the first and second moment of the ISI distribution at time $n + 1$ or at the next neuron layer, and ν_n^1 and ν_n^2 are the first and second moment of the ISI distribution at time n or at the current neuron layer. We currently have an analytical expression for G that has been derived from the IF equation, and we will apply it to our setup in subsequent work.

Formal Analysis

Our results are based on numerical simulations. We will try to develop an analytical understanding of a simplified version of this model. We will characterise the attractors of the system defined by Eq. (1.8), their domain of attraction, their stability, and the speed of convergence to these attractors as a function of various system parameters.

Hypothesis

We deduced a relation between error rate and reaction time. This relation can be used to test the hypothesis that the background noise activity of the brain controls the speed-accuracy trade off of decision making. Comparing our model characteristic of ER(RT) to the one of living beings, measured via psychophysical experiments, could support or invalidate our hypothesis.

1.4.4 Conclusion

Our model is a step toward the construction of a bridge between detailed neural models and real living behaviour such as sensory-based decision making, or between neurology and psychology. Computing with noise is also a new step toward less simplistic neural modeling, which takes into account the second-order statistics of spike trains. This more refined approach should give us insights into domains unreachable by the classic mean firing rate approaches.

References

1. Amit DJ, Brunel N 1997) Model of global spontaneous activity and local structured activity during delay periods in the cerebral cortex. *Cereb Cortex* 7:237–252.
2. Britten KH, Shadlen MN, Newsome WT, Movshon JA (1992) The analysis of visual motion : a comparison of neuronal and psychophysical performance. *J Neurosci* 12:2331–2355.

3. Deng Y, Williams P, Liu F and Feng J (2003) Discriminating between different input signals via single neuron activity. *Journal of Physics A: Mathematical and General* 36(50):12379–12398.
4. Feng J.(2001) Is the integrate-and-fire model good enough? A review. *Neural Networks* 14:955–975.
5. Feng J and Liu F (2002) A modeling study on discrimination tasks. *Biosystems* 67:67–73.
6. Gaillard B and Feng J (2005) Modelling a visual discrimination task. *Neurocomputing* 65-66:203–209.
7. Gaillard B, Feng J and Buxton H (2005) Population approach to a neural discrimination task. *Biological Cybernetics* 94(3):180–191
8. Gerstner W and Kistler W (2002) Spiking Neuron Models, Single Neurons, Populations, Plasticity. Cambridge University Press Cambridge, UK
9. Glimcher PW (2003) The neurobiology of visual-saccadic decision making. *Annu Rev Neurosci* 26:133–179.
10. Hubel DH and Wiesel TN (1962) Receptive fields, binocular interaction and functional architecture in the cat's visual cortex. *J Physiol (Lond)* 148:574–591.
11. Mountcastle VB (1957) Modality and topographic properties of single neurons of cat's somatosensory cortex. *J Neurophysiol* 20:408–434.
12. Platt ML and Glimcher PW (1999) Neural correlates of decision variables in parietal cortex. *Nature* 400:233–238.
13. Salinas E (2003) Background synaptic activity as a switch between dynamical states in a network. *Neural Computation* 15:1439–1475.
14. Shadlen MN and Gold JI(2004) The neurophysiology of decision making as a window on cognition. In: Gazzaniga (eds), *The Cognitive Neurosciences*, 3rd ed. MIT Press Cambridge, MA.
15. Shadlen MN and Newsome WT (2001) Neural basis of a perceptual decision in the parietal cortex (area LIP) of the rhesus monkey. *J Neurophysiol* 86:1916–1935.
16. Shadlen MN and Newsome WT (1996) Motion perception : seeing and deciding. *Proc Nat Acad Sci* 93:628–633.
17. Townsend JT and Ashby F (1983) The stochastic modeling of elementary psychological processes. Cambridge University Press, Cambridge, MA.
18. Tuckwell H(1988) Introduction to Theoretical Neurobiology, vol. 2. Cambridge University Press, Cambridge, MA.
19. VanRullen R and Koch C(2003) Is perception discrete or continuous? *Trends Cog Sci* 7(5):207–213.
20. Wang XJ (2002) Probabilistic decision making by slow reverberation in cortical circuits. *Neuron* 36:955–968.
21. Zohary E, Shadlen MN and Newsome WT (1994) Correlated neuronal discharge rate and its implications for psychophysical performance. *Nature* 370:140–143.